Supplementary Information

Single-atom Ni encapsulated in N-doped porous carbon microspheres for enhanced catalytic transfer hydrogenation

Sijia Pei,[a] Yuanyuan Yue,[a] Wenjun Du,[a] Liwei Niu,[b,*] Zhuo Li,[a] Dawei Liu,[a,*]

Yunteng Qu,[c] Long Xu,[a,*] Xiaoxun Ma[a]

[a] School of Chemical Engineering, Northwest University, International Science & Technology Cooperation Base of Most for Clean Utilization of Hydrocarbon Resources, Chemical Engineering Research Center of the Ministry of Education for Advanced Use Technology of Shanbei Energy, Shaanxi Research Center of Engineering Technology for Clean Coal Conversion, Xi'an 710069, China

[b] School of Chemistry and Chemical Engineering, Qilu University of Technology (Shandong Academy of Sciences), Jinan, 250353, China

[c] International Collaborative Center on Photoelectric Technology and Nano Functional Materials, Institute of Photonics & Photon-Technology, Northwest University, Xi'an 710069, China

Corresponding Author：

Liwei Niu, E-mail address: niuliwei@qlu.edu.cn

Dawei Liu, E-mail address: dwliu@nwu.edu.cn

Long Xu, E-mail address: longxuxulong@163.com

Table of Contents

1. Supplementary Experimental section

1.1 Chemicals

Melamine (98%), formaldehyde (37 wt% aqueous solution), toluene (99%), D-(+)-glucose (99%) and nickel (II) nitrate hexahydrate (99%) were purchased from Tianjin Kemiou Chemical Reagent Co., Ltd. F127, nitroarenes, N-heterocycles and organic solvents were purchased from Shanghai Aladdin Biochemical Technology Co., Ltd. All reagents were used as received without further purification.

1.2 Emulsifier preparation

Typically, 24 mL of n-hexanol, 115.5 mL of cyclohexane, 28.5 mL of TX-10, and 5.1 g of deionized water were added to a round-bottomed flask and stirred at room temperature for 30 min. Then, 9.8138 g of tetraethyl orthosilicate (TEOS) was added dropwise, and the mixture was stirred for an additional 5 h. Subsequently, 1.5 mL of aqueous ammonia solution was added, and the reaction mixture was stirred for 18 h. The reaction was then terminated by adding 15 mL of ethanol. The resultant suspension was centrifuged, and the precipitate was washed five times with ethanol, followed by drying at 100 ^{o}C for 4 h, obtaining silica nanospheres with diameters in the range of approximately 60-80 nm. Next, 1.5 g of the as-prepared silica nanospheres was dispersed in 40 mL of toluene. A mixture containing 4.5 mmol of trimethoxymethylsilane $(MeO)_3SiCH_3$ and 4.5 mmol of triethylamine $(C_2H_5)_3N$ was then added. The reaction mixture was refluxed at 120 ^{o}C for 4 h. The solid product was collected by centrifugation, washed with toluene, and dried under vacuum to yielding methyl-modified silica particles, which were used as particle emulsifier.

2. Supplementary Figures

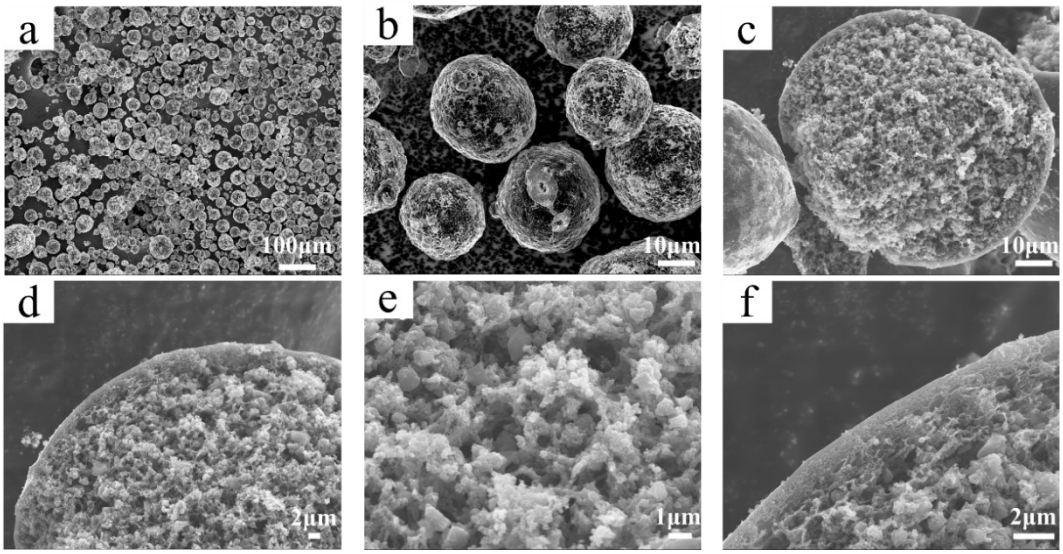

Fig. S1. SEM images of 1.3Ni@NHC-500

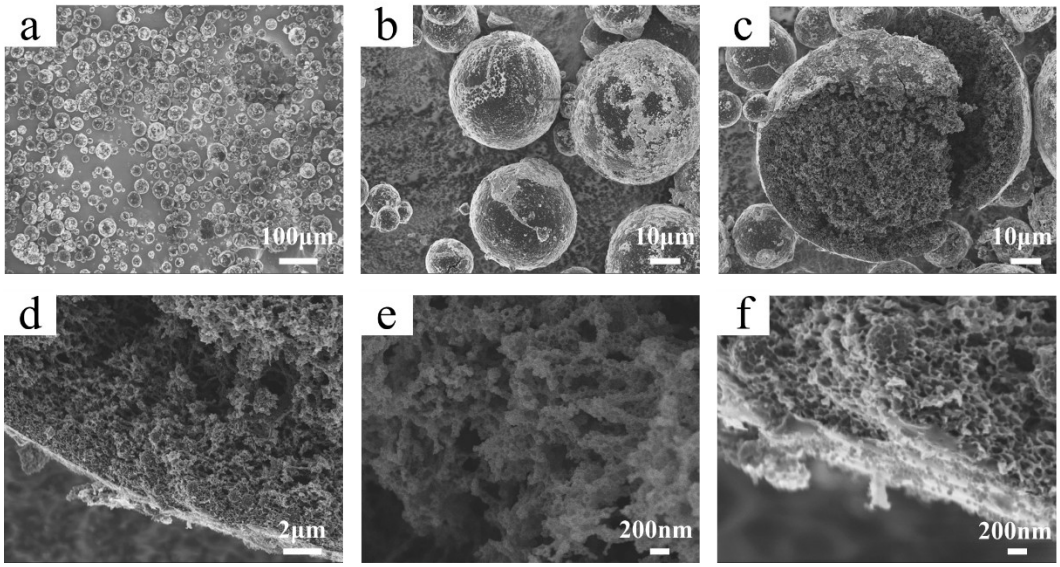

Fig. S2. SEM images of 1.3Ni@NHC-700

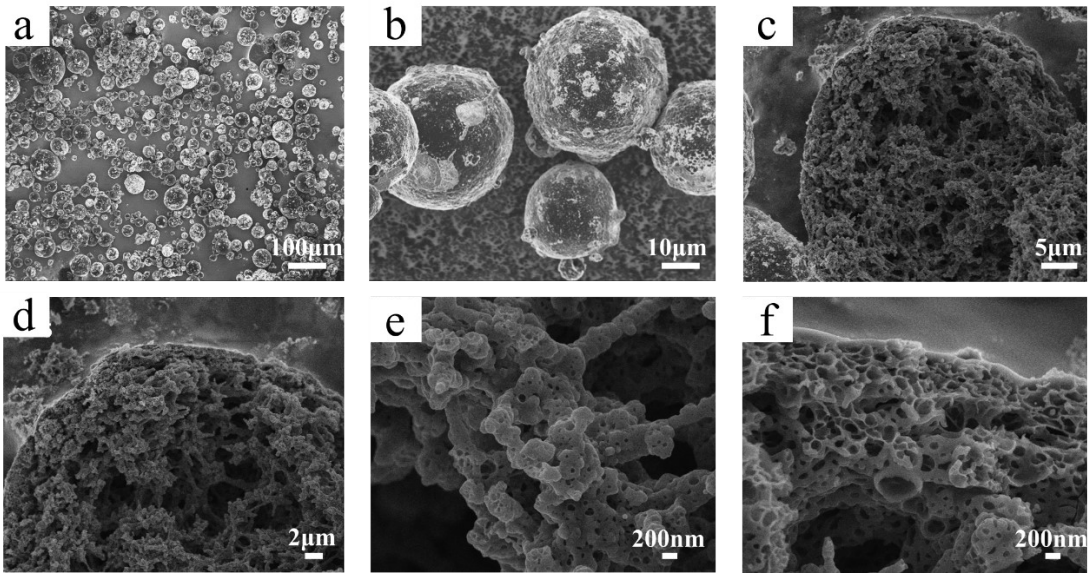

Fig. S3. SEM images of 1.3Ni@NHC-800

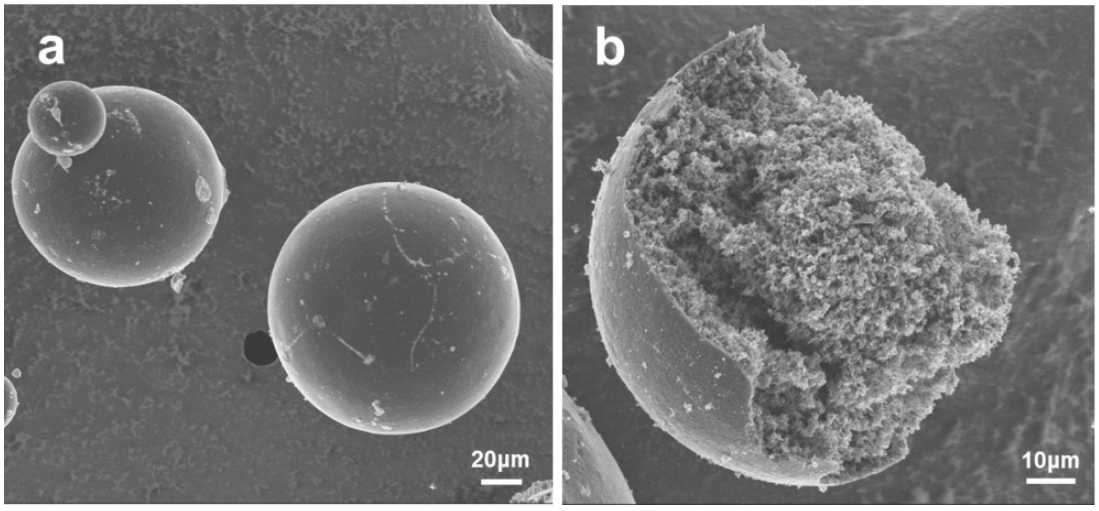

Fig. S4. SEM images of 4.9Ni@NHC-600

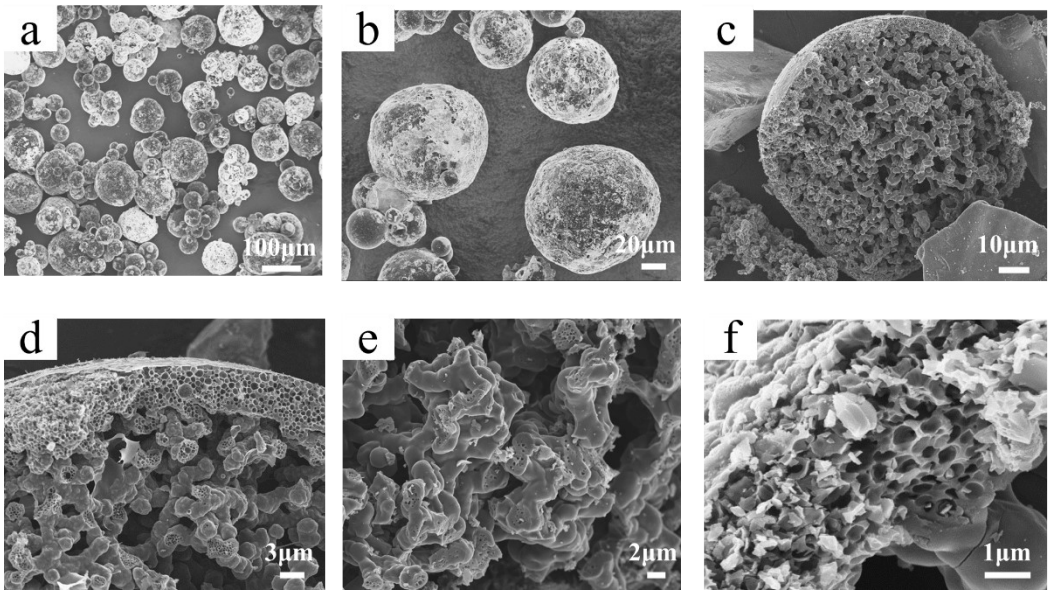

Fig. S5. SEM images of NHC-600

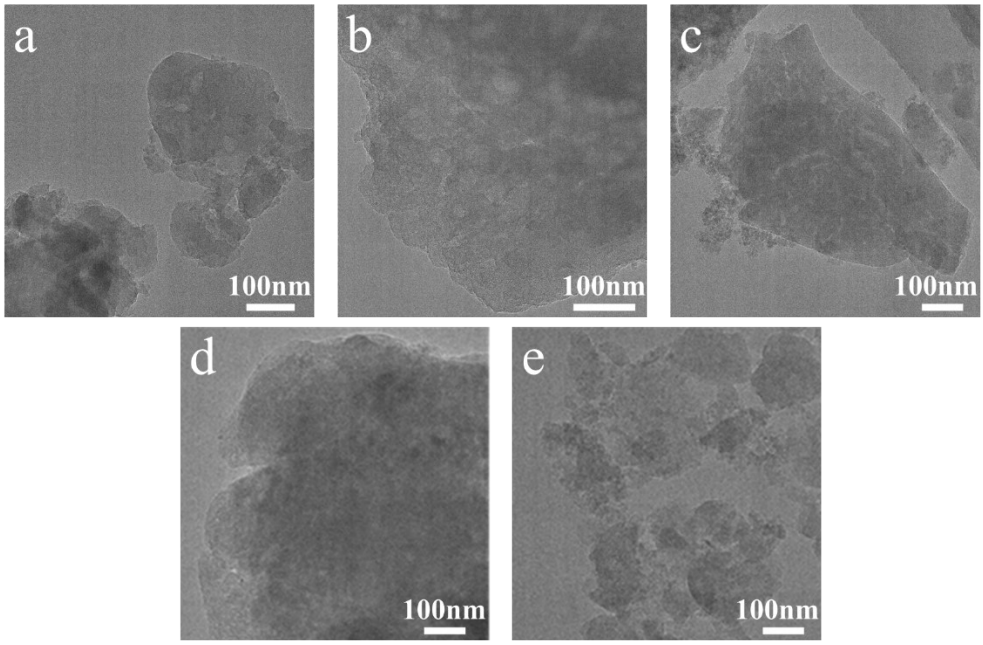

Fig. S6. TEM images of NHC-600 and 1.3Ni@NHC-T. (a) 1.3Ni@NHC-500, (b) 1.3Ni@NHC-600, (c) 1.3Ni@NHC-700, (d) 1.3Ni@NHC-800, (e) NHC-600

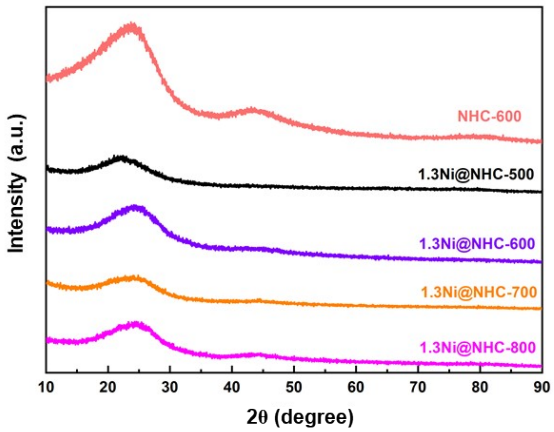

Fig. S7. XRD patterns of NHC-600 and 1.3Ni@NHC-T

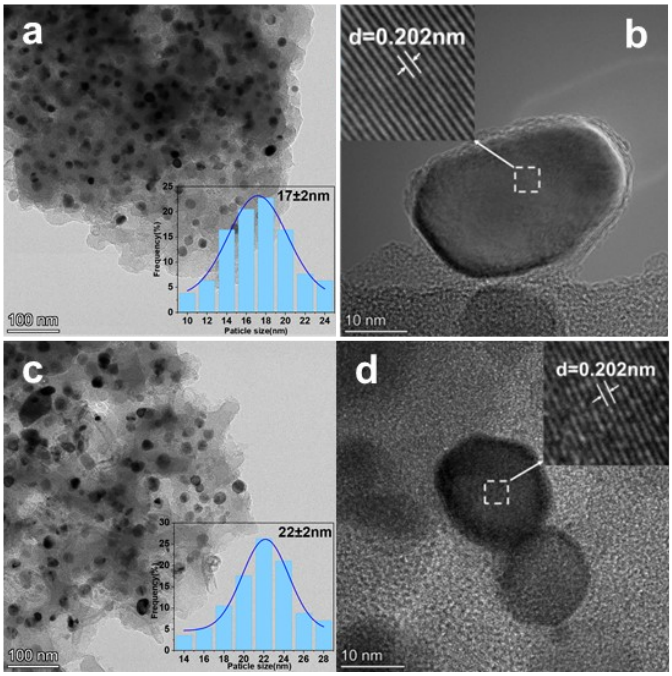

Fig. S8. (a-b) TEM images of 4.9Ni@NHC-600, (c-d) TEM images of 22Ni@NHC-600

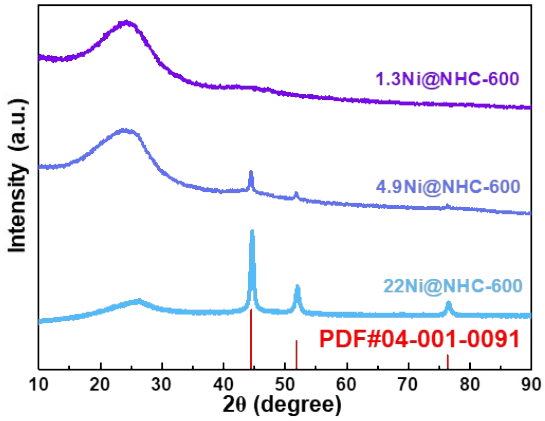

Fig. S9. XRD patterns of xNi@NHC-600

As shown in Fig. S9, diffraction peaks at 2θ = 44.5°, 51.8°, and 76.4° could be assigned to the (111), (200), and (220) planes of metallic Ni nanocrystal, confirming the presence of Ni NPs in the 4.9Ni@NHC-600 and 22Ni@NHC-600 catalysts.

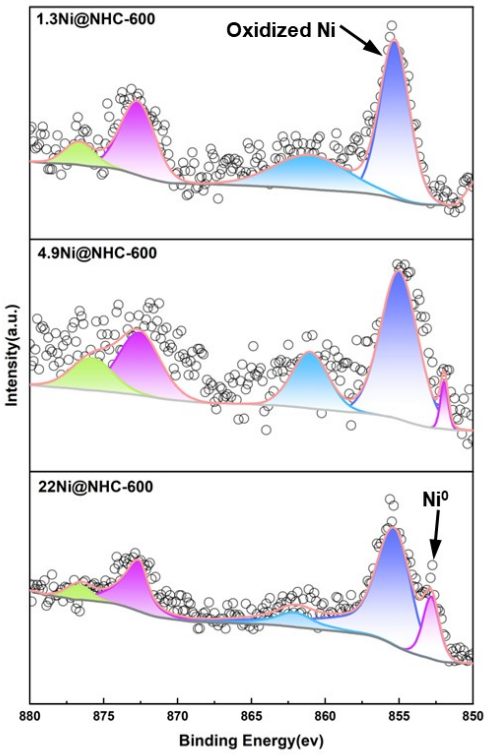

Fig. S10. XPS Ni2*p* spectra of xNi@NHC-600

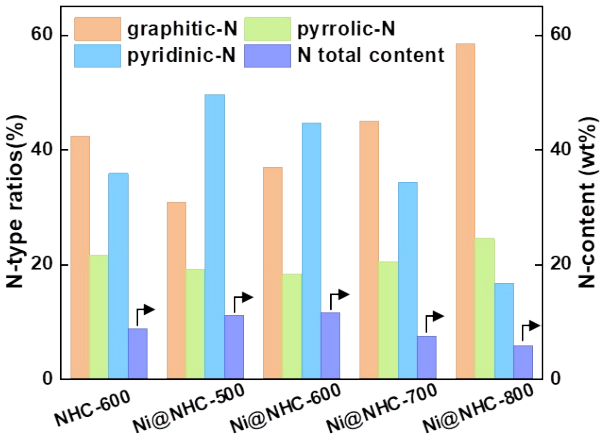

Fig. S11. Quantitative analysis of N species in NHC-600 and 1.3Ni@NHC-T

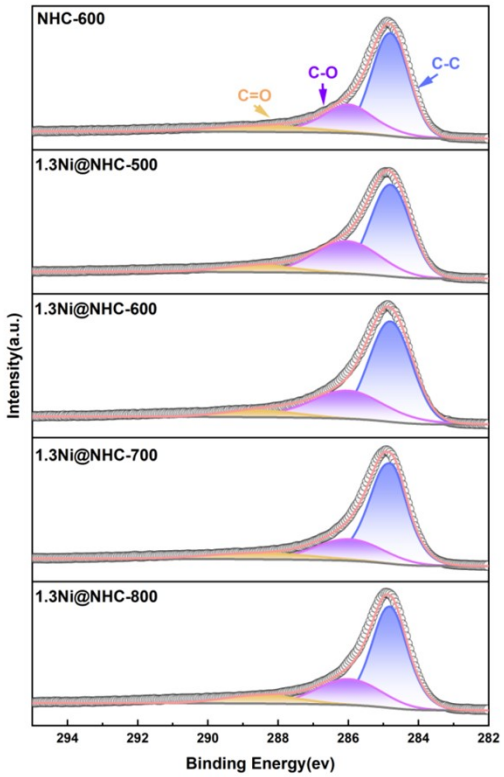

Fig. S12. C1*s* spectra of NHC-600 and 1.3Ni@NHC-T

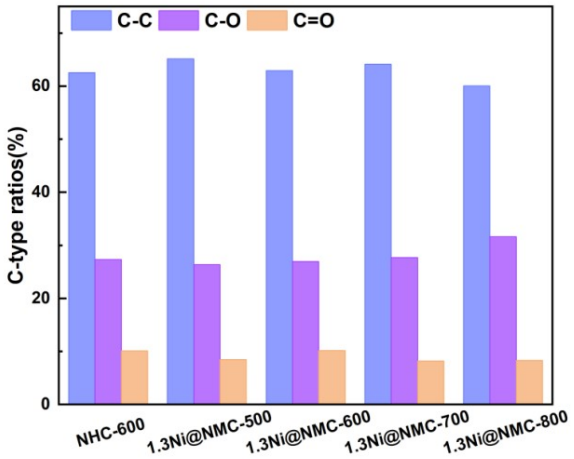

Fig. S13. Quantitative analysis of C species in NHC-600 and 1.3Ni@NHC-T

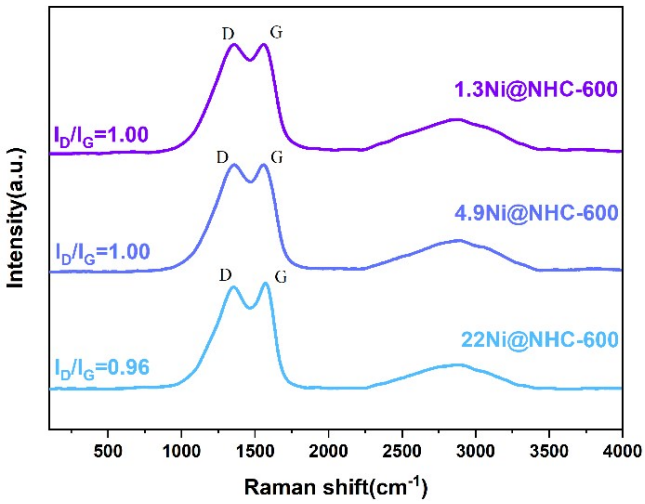

Fig. S14. Raman spectra of xNi@NHC-600

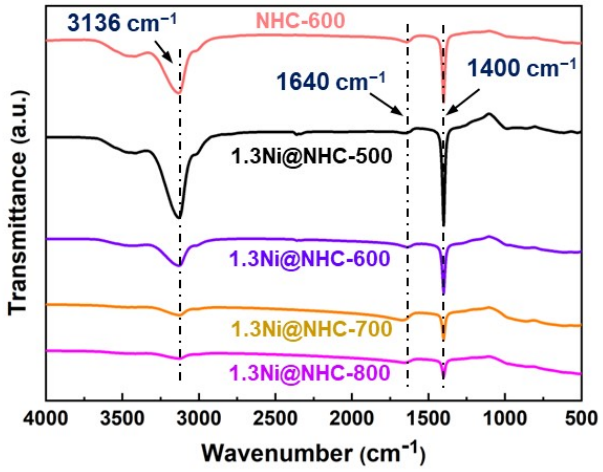

Fig. S15. FT-IR spectrum of NHC-600 and 1.3Ni@NHC-T

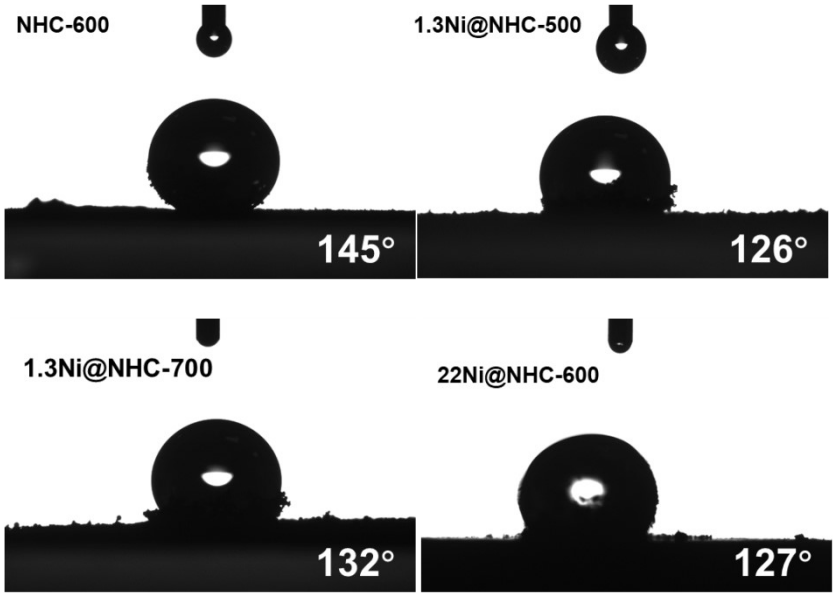

Fig. S16. Water contact angles of various catalysts

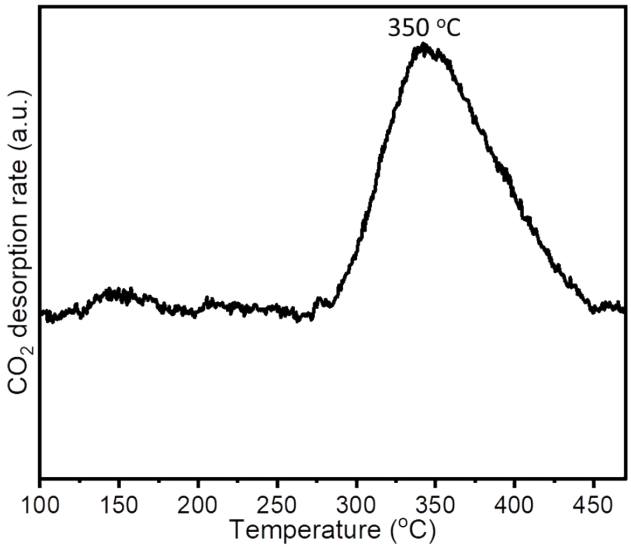

Fig. S17. CO_2-TPD of NHC-600

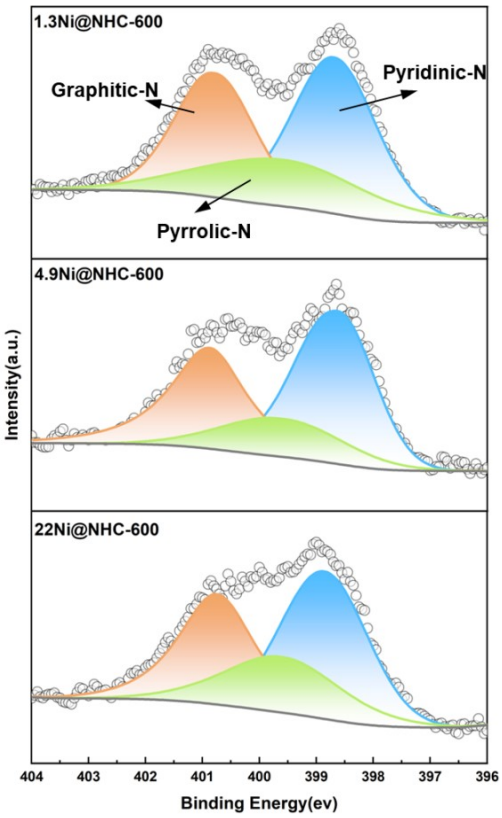

Fig. S18. XPS N1*s* spectra of xNi@NHC-600

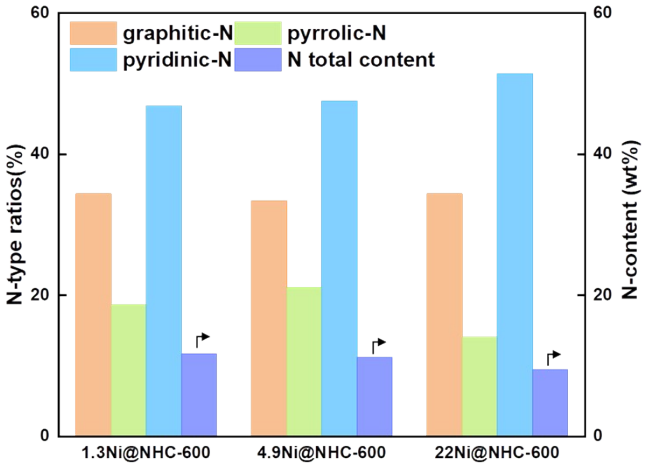

Fig. S19. Quantitative analysis of N species in xNi@NHC-600

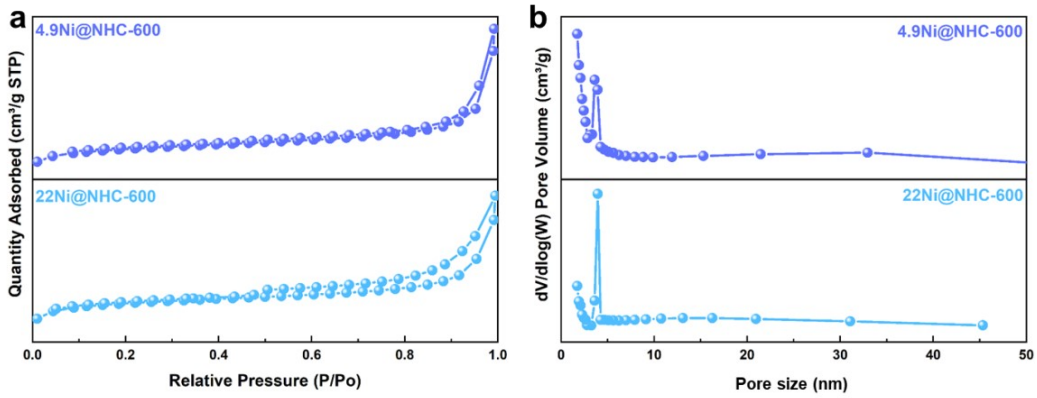

Fig. S20. (a) N_2 adsorption-desorption isotherms and (b) pore size distribution curves of xNi@NHC-600

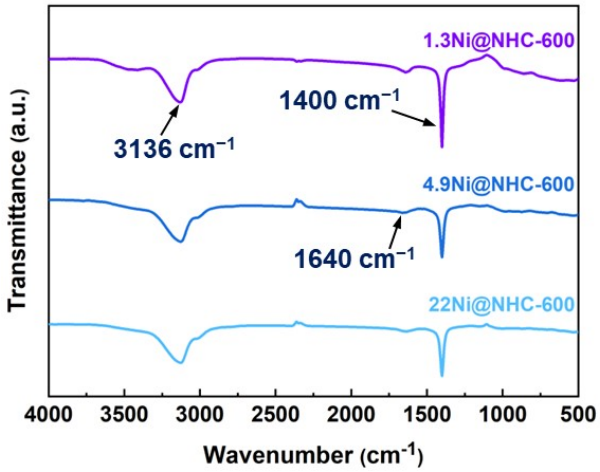

Fig. S21. FT-IR spectrum of xNi@NHC-600

FT-IR analysis of xNi@NHC-600 catalysts suggests that no significant changes in the overall peak pattern, indicating that the content of Ni does not significantly alter the surface functional group composition.

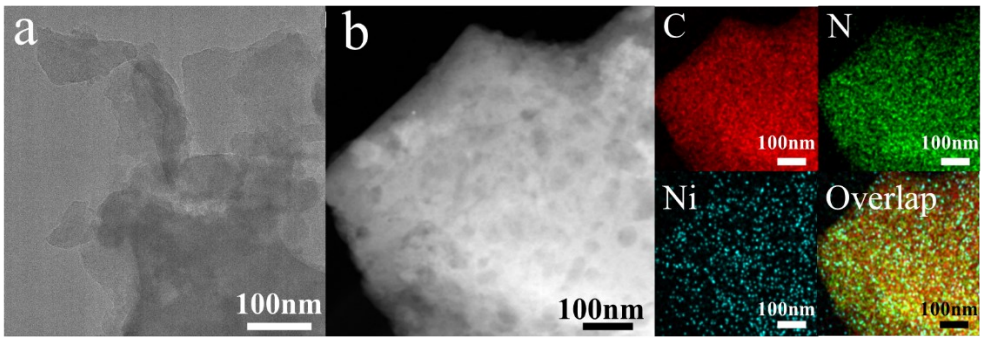

Fig. S22. (a) TEM image of 1.3Ni@NHC-600 after 9 cycles, (b) HAADF-TEM image and corresponding elemental mappings

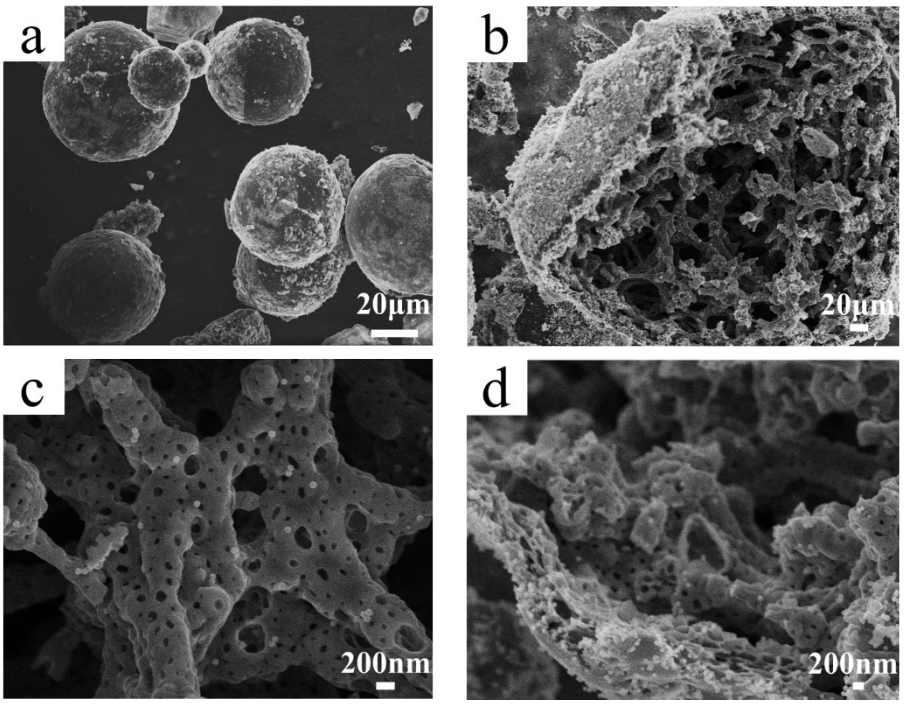

Fig. S23. SEM images of 1.3Ni@NHC-600 after 9 cycles

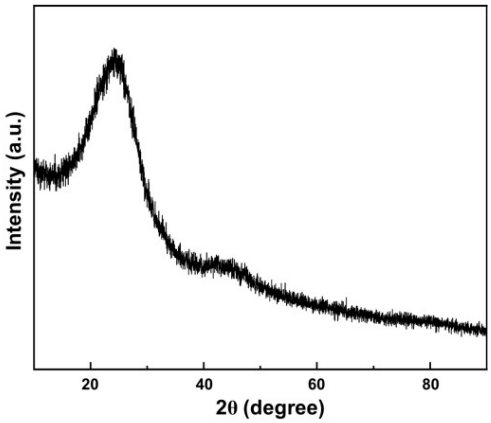

Fig. S24. XRD spectrum of 1.3Ni@NHC-600 after 9 cycles

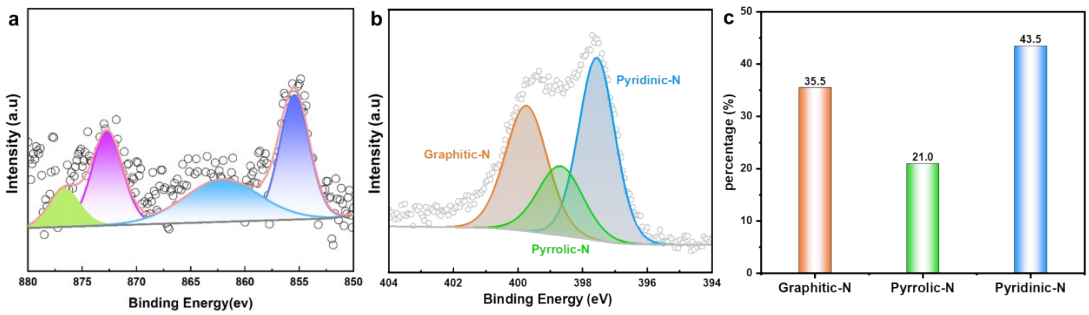

Fig. S25. XPS results of 1.3Ni@NHC-600 after 9 cycles. (a) Ni2*p* spectrum, (b) N1*s* spectrum, and (c) percentages of N-species

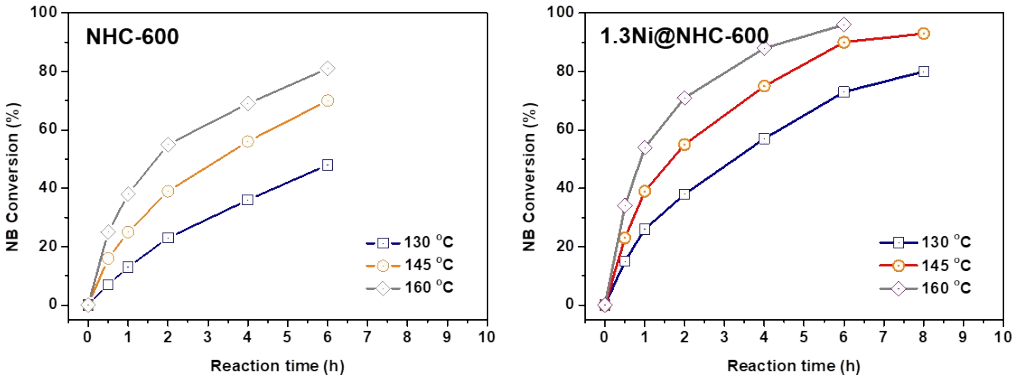

Fig. S26. Nitrobenzene (NB) conversions as a function of reaction time over NHC-600 and 1.3Ni@NHC-600

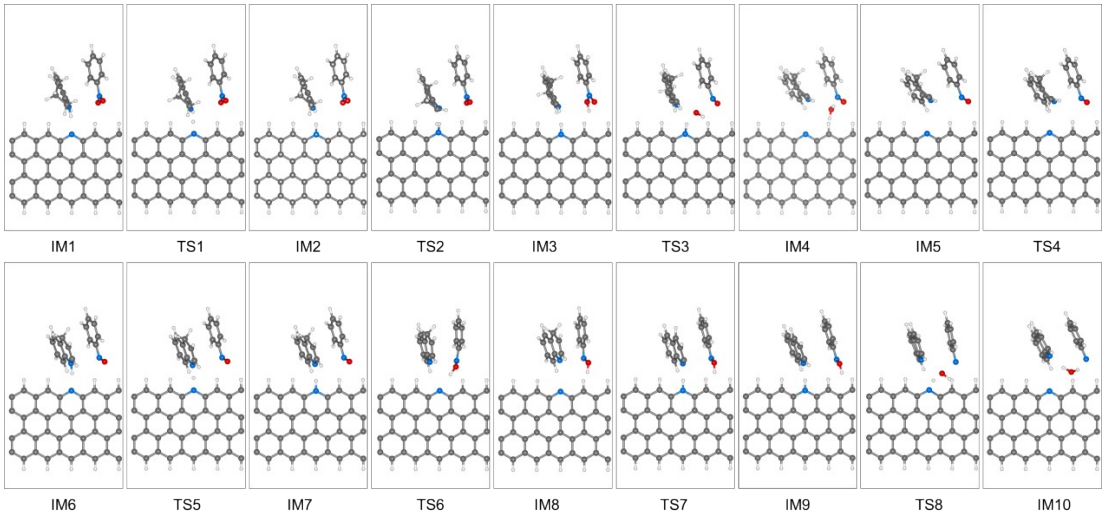

Fig. S27. Structural evolution of 1,2,3,4-tetrahydroquinoline dehydrogenation and nitrobenzene hydrogenation on the NHC-600 catalyst

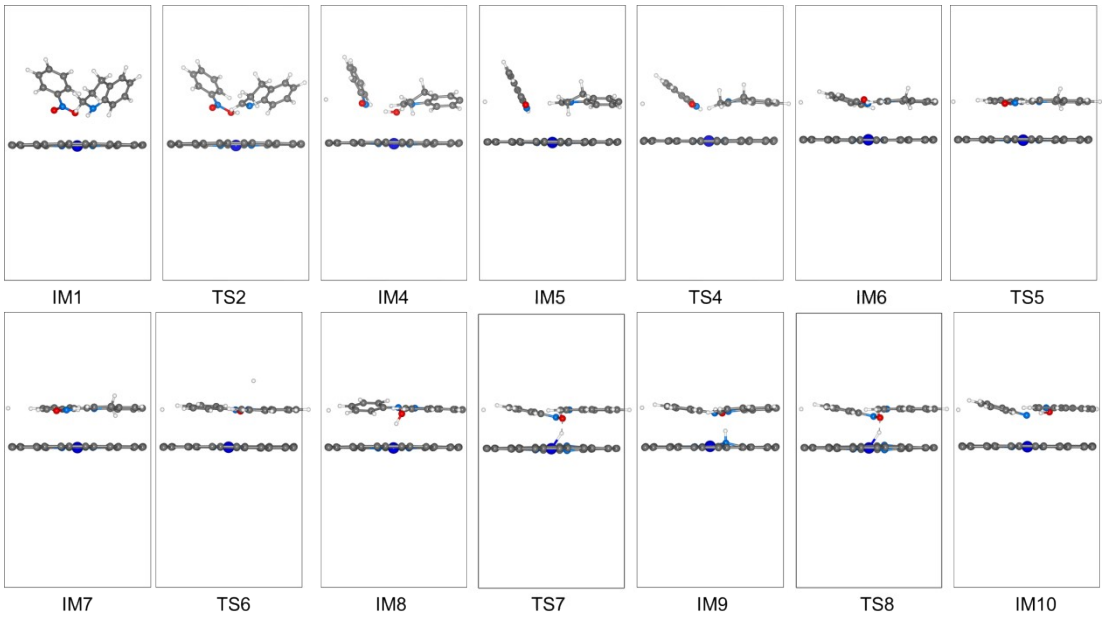

Fig. S28. Structural evolution of 1,2,3,4-tetrahydroquinoline dehydrogenation and nitrobenzene hydrogenation on the 1.3Ni@NHC-600 catalyst

3. Supplementary Tables

Table S1. Elemental analysis of various catalysts

Catalysts	N (wt%)	C (wt%)	Ni[a] (wt%)	N (at%)	C (at%)	Ni (at%)
NHC-600	8.81	66.86	—	10.15	89.85	—
1.3Ni@NHC-500	11.19	36.84	1.59	20.51	78.79	0.70
1.3Ni@NHC-600	11.71	60.11	1.36	14.25	85.35	0.40
1.3Ni@NHC-700	7.62	62.17	1.30	9.47	90.14	0.39
1.3Ni@NHC-800	5.83	68.66	1.16	6.76	92.92	0.32
4.9Ni@NHC-600	11.16	66.15	4.94	12.47	86.21	1.32
22Ni@NHC-600	11.12	61.17	22.15	12.67	81.30	6.03
1.3Ni@NHC-600[b]	11.69	60.12	1.33	14.23	85.38	0.39

[a] Results determined by ICP-OES. [b] After nine cycles. The atomic ratio of N, C and Ni elements is calculated from the results of ICP.

Table S2. EXAFS fitting parameters at the Ni K-edge for 1.3Ni@NHC-600 and 4.9Ni@NHC-600

Catalysts	Shell	N[a]	R (Å) [b]	σ^2 (Å$^2\cdot10^{-3}$) [c]	ΔE_0 (eV) [d]	R-factor
1.3Ni@NHC-600	Ni-N/O	3.9±0.2	1.88±0.02	5.1±3.0	-1.4±0.2	0.015
4.9Ni@NHC-600	Ni-N/O	2.1±0.2	1.79±0.02	5.6±3.0	-1.9±0.2	0.012
	Ni-Ni	5.9±0.2	2.46±0.02	6.3±3.0	-2.2±0.2	

[a] N: coordination numbers; [b] R: bond distance; [c] σ^2: Debye-Waller factors; [d] ΔE_0: the inner potential correction.

Table S3. Textural properties of various catalysts

Catalysts	S_{BET} (m^2/g)	Pore volume (cm^3/g)	Pore size (nm)
NMC-600	320	0.26	13.5
1.3Ni@NMC-500	290	1.09	18.1
1.3Ni@NHC-600	324	0.48	16.3
1.3Ni@NMC-700	328	0.53	16.6
1.3Ni@NMC-800	294	0.45	13.5
4.9Ni@NMC-600	361	0.35	3.6
22Ni@NMC-600	347	0.26	3.9

Table S4. Transfer hydrogenation reaction between nitrobenzene and 1,2,3,4-tetrahydroquinoline over various catalysts

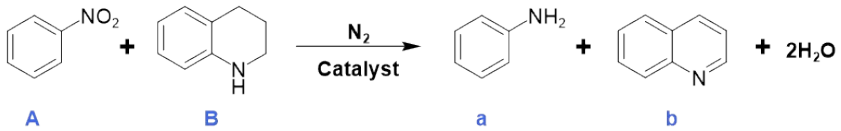

A B a b

Entry	Solvent	Con. of A (%)	Con. of B (%)	Yield of a (%)	Yield of b (%)
1	Blank	<1	<1	—	—
2	SiO_2	<1	<1	—	—
3	NHC-600	73	72	73	72
4	NHC-700	56	57	56	57
5	NHC-800	39	39	39	39
6	NHC-600[a]	48	51	48	51
7	1.3Ni@NHC-600[a]	86	86	86	86
8	1.3Ni@NHC-600[b]	87	88	87	88
9	1.3Ni@NHC-600[c]	<1	—	—	—
10	0.8Ni@NHC-600[d]	80	80	80	80
11	Ni/NHC-600[e]	74	73	74	73

[a] Catalyst pyrolyzed under N_2 atmosphere.

[b] The reaction was scaled up 20 times.

[c] The reaction was carried out in water as the solvent, in the absence of 1,2,3,4-tetrahydroquinoline.

[d] Ni content is determined to be 0.8wt% by ICP analysis.

[e] Catalyst prepared via impregnation with 1.3 wt% Ni content.

Reaction conditions: nitrobenzene (0.5 mmol), 1,2,3,4-tetrahydroquinoline (0.75 mmol), catalyst (60 mg), H_2O (3 mL), 145 °C, 6 h, N_2.

Table S5. Performance comparison of reported catalysts in transfer hydrogenation reaction between nitrobenzene and 1,2,3,4-tetrahydroquinoline

Catalysts	$W_{cat.}$ (mg)	T (°C)	n_{NB} (mmol)	t (h)	Aniline yield (%)	Quinoline yield (%)	R^a	TOF[b]	Ref.
1.3Ni@NHC-600 (1.3 wt% Ni)	60	145	0.5	6	90	90	1.250	6.27	This work
NHC-600	60	145	0.5	6	73	72	1.014	—	This work
Co/mNC-500 (14.08 wt%Co)	20	160	0.4	24	91	96	0.758	0.35	[1]
Ni@NCF-700 (50.13 wt%Ni)	50	145	0.5	18	97	96	0.550	0.065	[2]
Co-N-C-900 (1.12 wt% Co)	50	145	0.125	24	98	98	0.102	0.532	[3]
$ONC_{0.4}$-800	20	180	0.4	24	90	91	0.750	—	[4]
FBC-850	50	140	0.5	14	94	92	0.671	—	[5]

[a] Reaction activity (R) was calculated based on catalyst amount and nitrobenzene (NB) conversion, $mmol_{NB}/(g_{cat.}\cdot h)$

[b] TOF was calculated based on the total metal molar amounts in the catalyst and nitrobenzene conversion, h^{-1}

Table S6. Bond lengths of N-H and Ni-H in TS7 and TS8

Catalysts	Bond	Bond length (TS7)	Bond length (TS8)
NHC-600	N-H	1.05 Å	1.25 Å
1.3Ni@NHC-600	Ni-H	2.48 Å	1.67 Å
	N-H	1.27 Å	1.50 Å

References

[1] Lu, X.; Qin, J.; Xian, C.; Nie, J.; Li, X.; He, J. Cobalt Nanoparticles Supported on Microporous Nitrogen-Doped Carbon for Efficient Catalytic Transfer Hydrogenation Reaction between Nitroarenes and N-Heterocycles. Catal. Sci. Technol., 2022, 12, 5549–5558.

[2] Pang, S.; Zhang, Y.; Su, Q.; Liu, F.; Xie, X.; Duan, Z.; Zhou, F.; Zhang, P.; Wang, Y. Superhydrophobic Nickel/Carbon Core–Shell Nanocomposites for the Hydrogen Transfer Reactions of Nitrobenzene and N-Heterocycles. Green Chem. 2020, 22, 1996–2010.

[3] Xu, D.; Liu, R.; Li, J.; Zhao, H.; Ma, J.; Dong, Z. Atomically Dispersed Co-N_4 Sites Anchored on N-Doped Carbon for Aqueous Phase Transfer Hydrogenation between Nitroarenes and Saturated N-Heterocycles. Appl. Catal. B: Environ. 2021, 299, 120681.

[4] Lu, X.; He, J.; Huang, L.; Qin, J.; Ma, Y.; Liu, X.; Zhao, W.; Liu, B.; Zhang, Z. Synergetic Roles of Pyridinic Nitrogen and Carbonyl Sites in Nitrogen-Doped Carbon for the Metal-Free Transfer Hydrogenation Reactions. Appl. Catal. B: Environ. 2023, 324, 122277.

[5] Pang, S.; Xi, X.; Liu, S.; Wang, B.; Liang, J.; Zhang, Y.; Chen, Q.; Su, Q.; Wang, Y. Superhydrophobic Biochars as Catalysts for Efficient Hydrogen Transfer in N-heterocycles and Nitrobenzene Reactions. Fuel, 2024, 372, 132224.

4. Supplementary Gas Chromatography and Mass Spectrometry

GC spectrum:

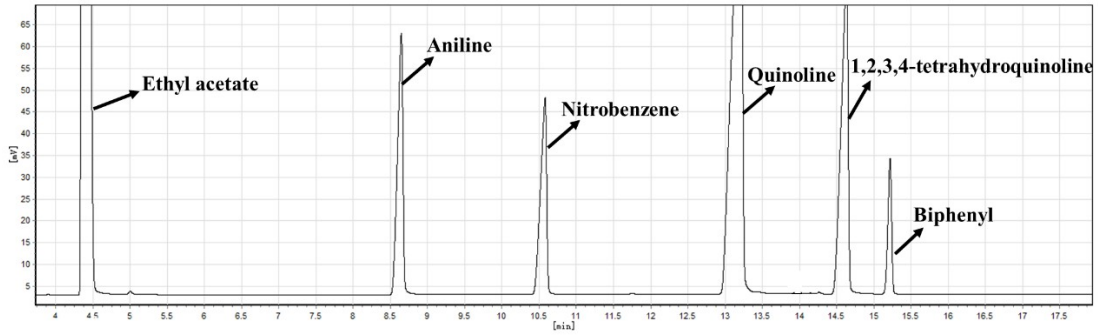

Mass spectrometry:

3a: Aniline

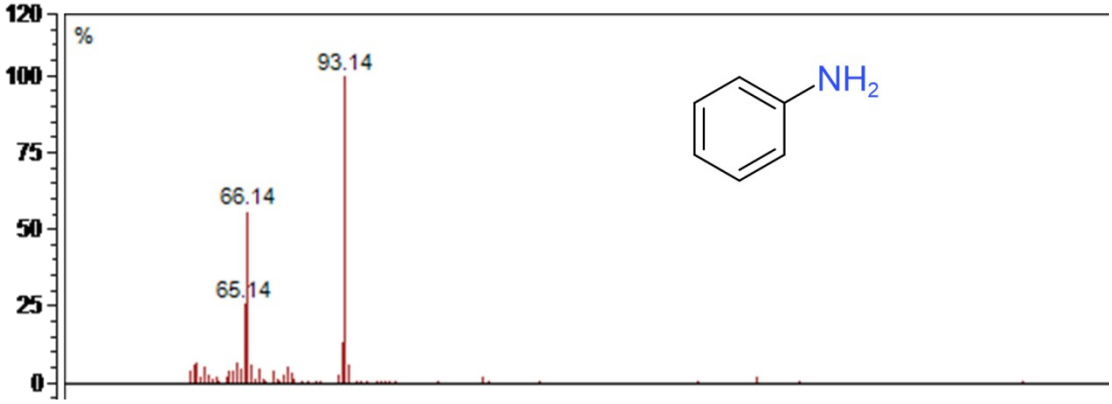

3b: 1-Amino-2-methylbenzene

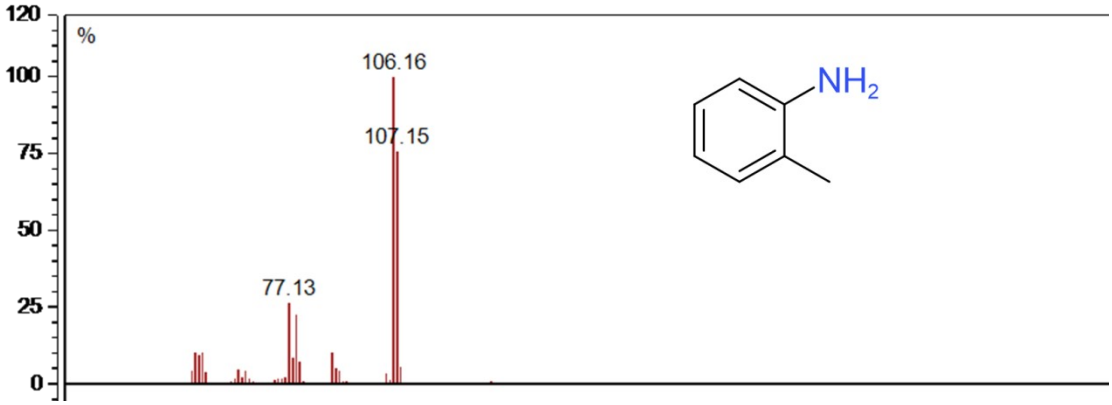

3c: 3-Aminotoluene

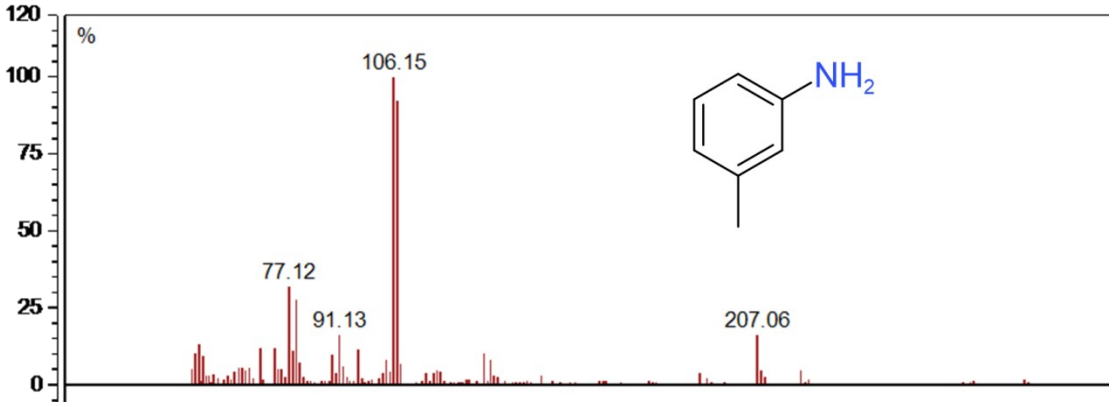

3d: 4-Aminotoluene

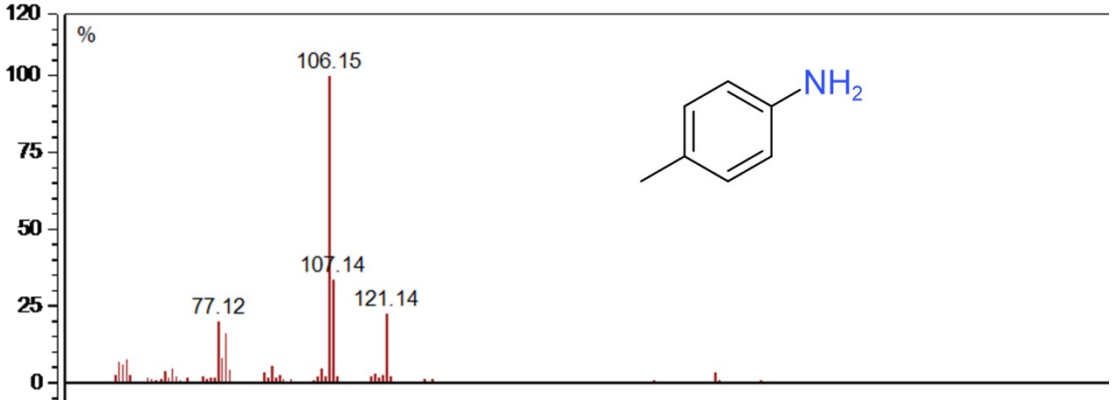

3e: 4-Ethylphenethylamine

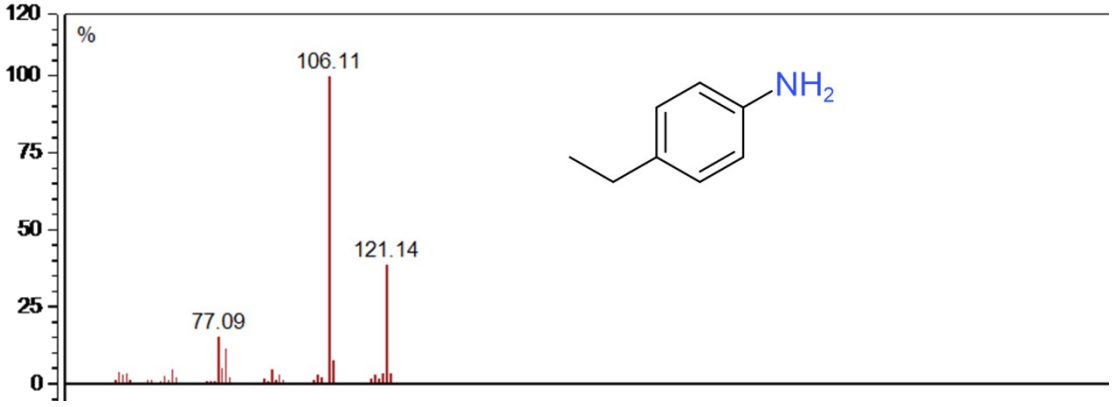

3f: 1,2-Benzenediamine

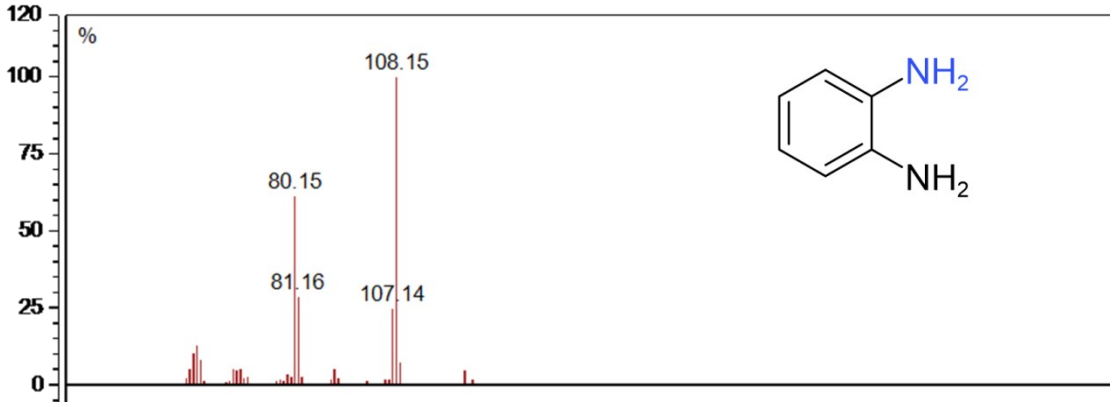

3g: 1,4-Benzenediamine

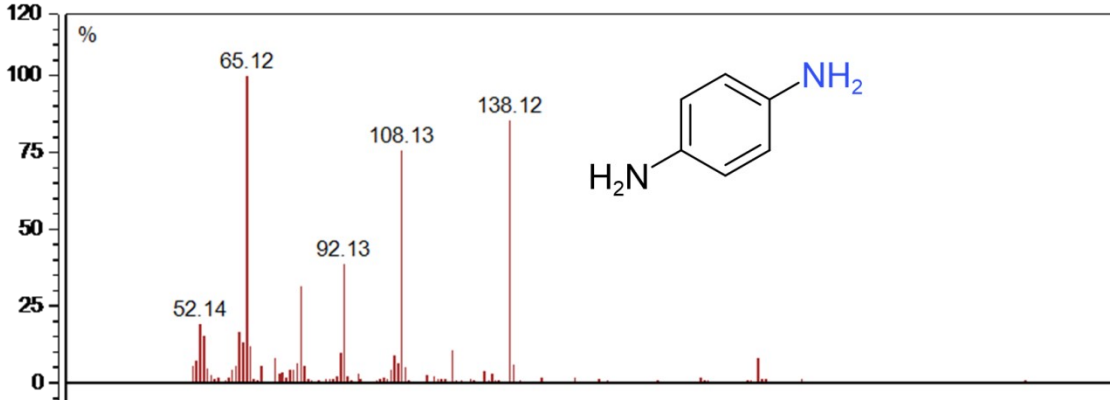

3i: 2-Chloroaniline

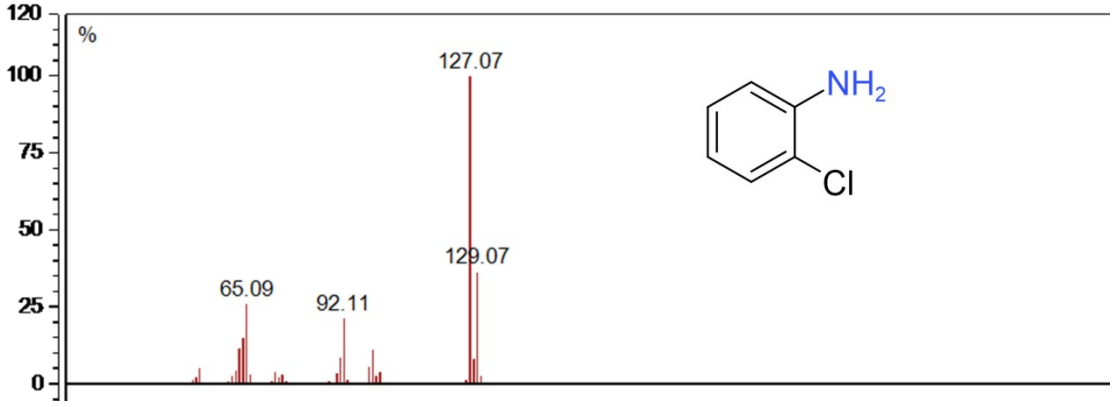

3j: 3-Chloroaniline

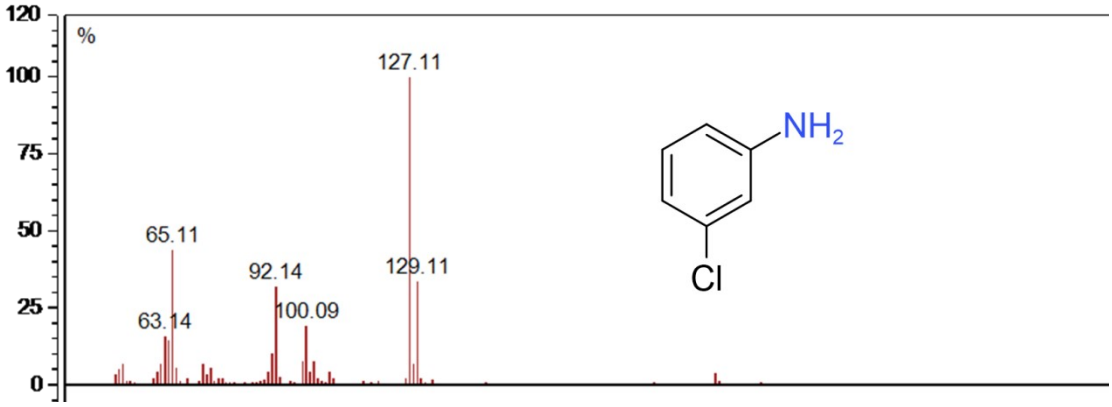

3k: 4-Chloroaniline

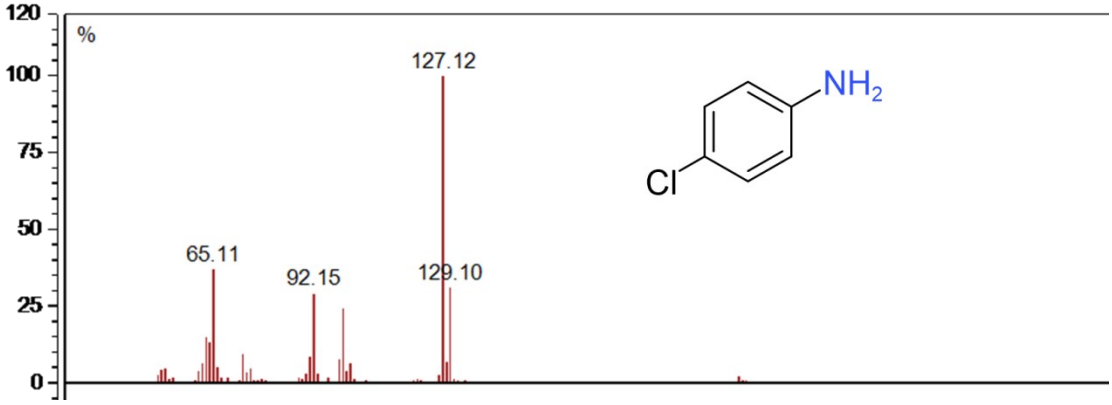

3l: 2-Fluoroaniline

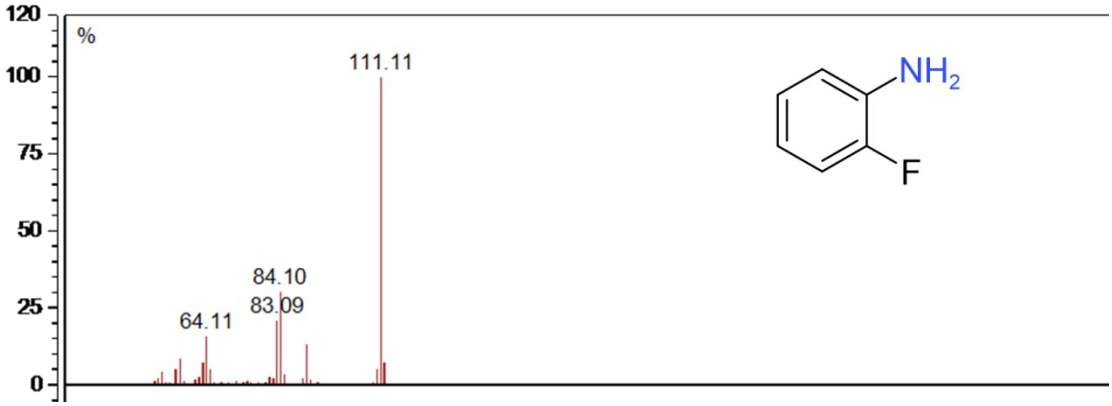

3m: 3-Fluoroaniline

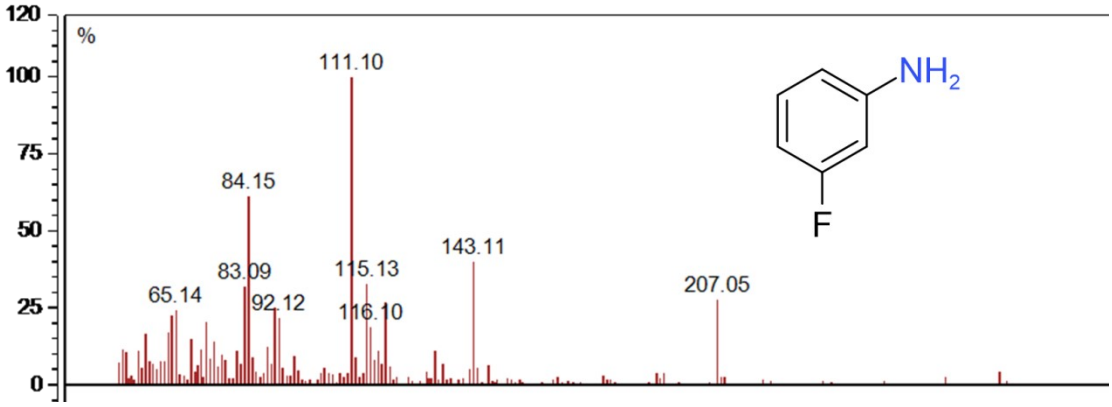

3n: 4-Bromoaniline

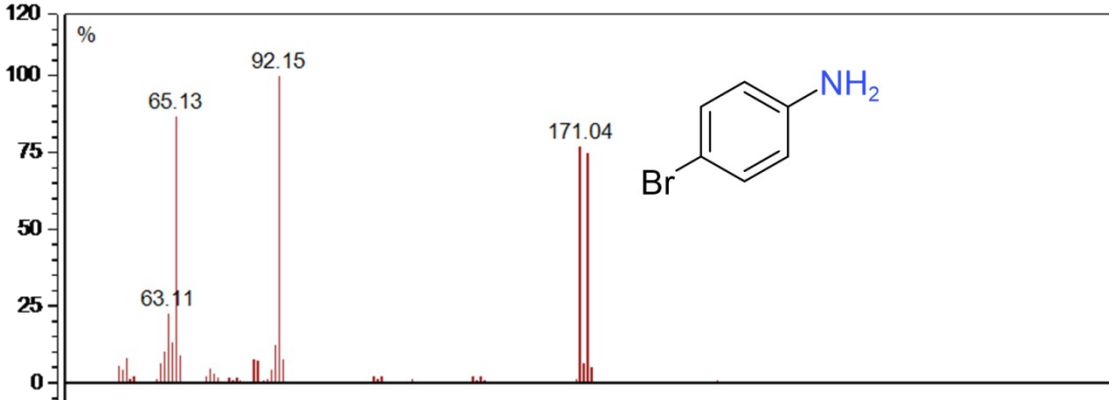

3o: 4-Aminobenzaldehyde

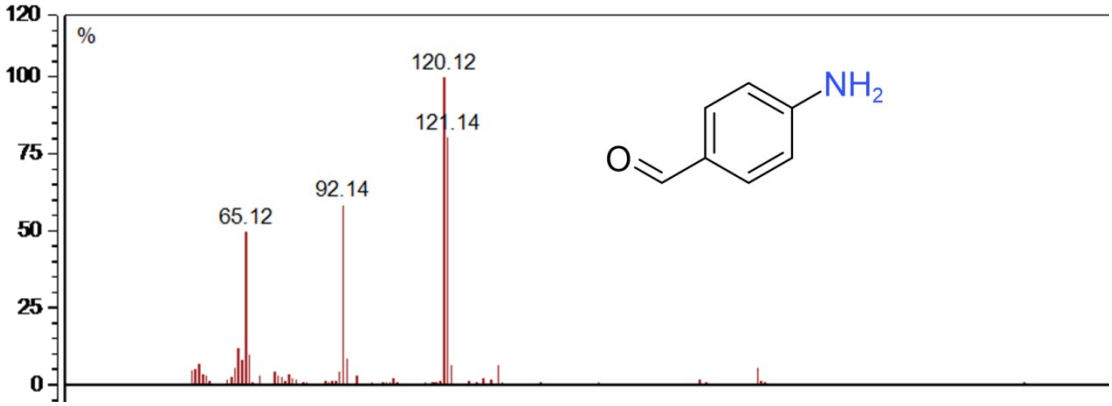

3p: 4-Aminobenzonitrile

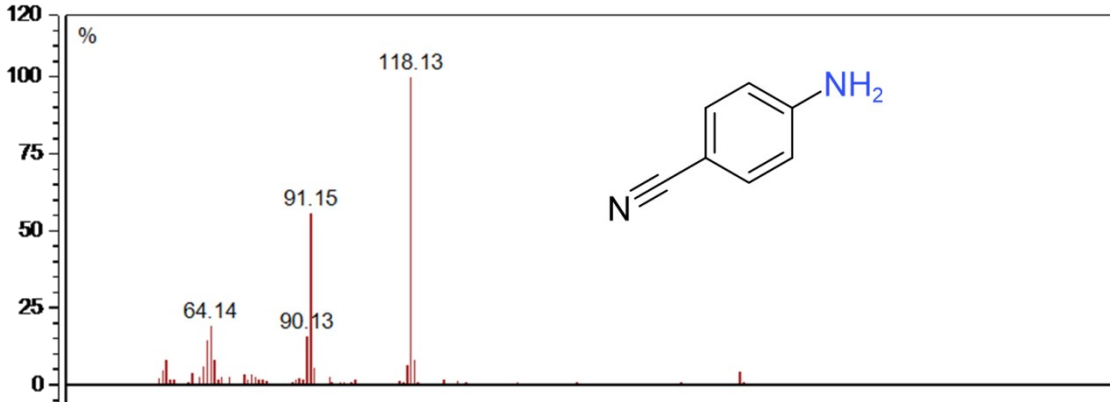

3q: 4-Aminoacetophenone

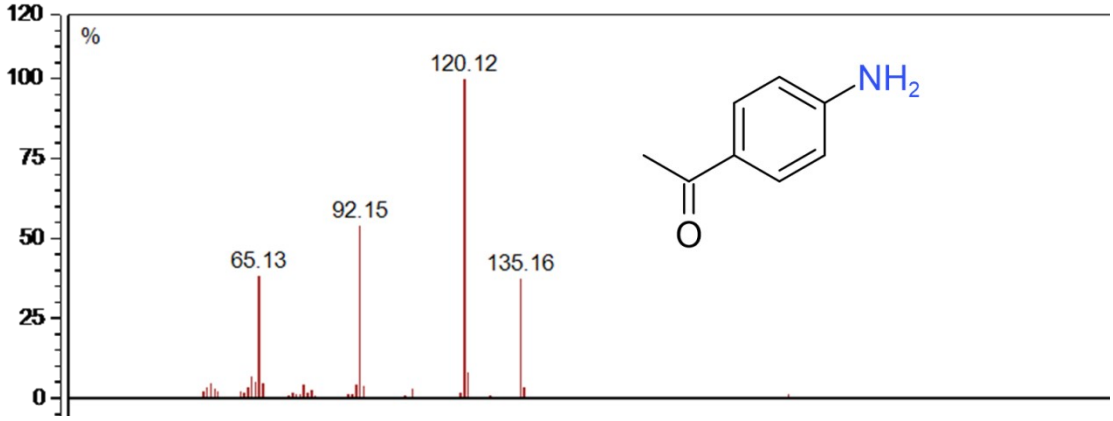

3r: Benzocaine

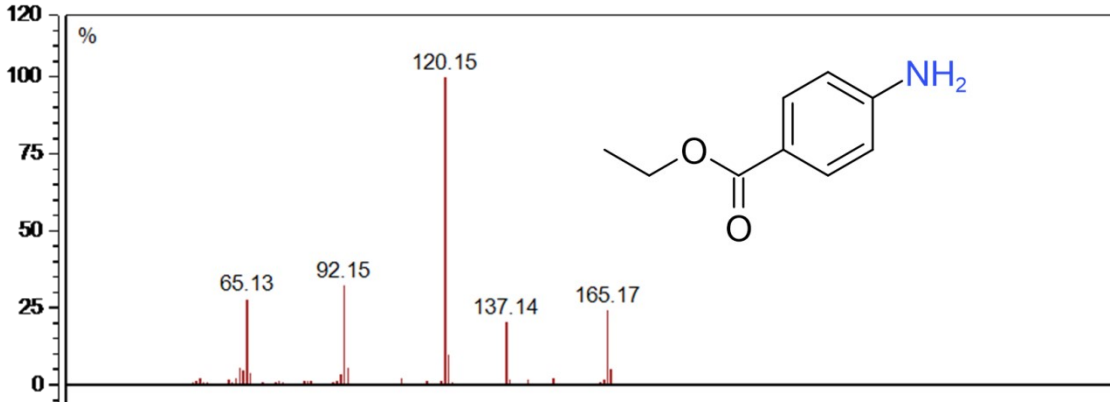

3s: 2-Aminoacetophenone

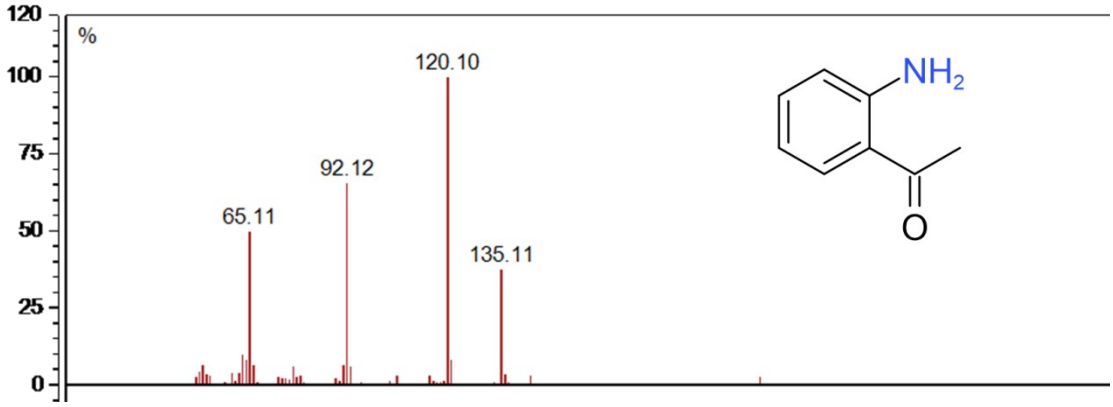

3t: 1-naphthylamine

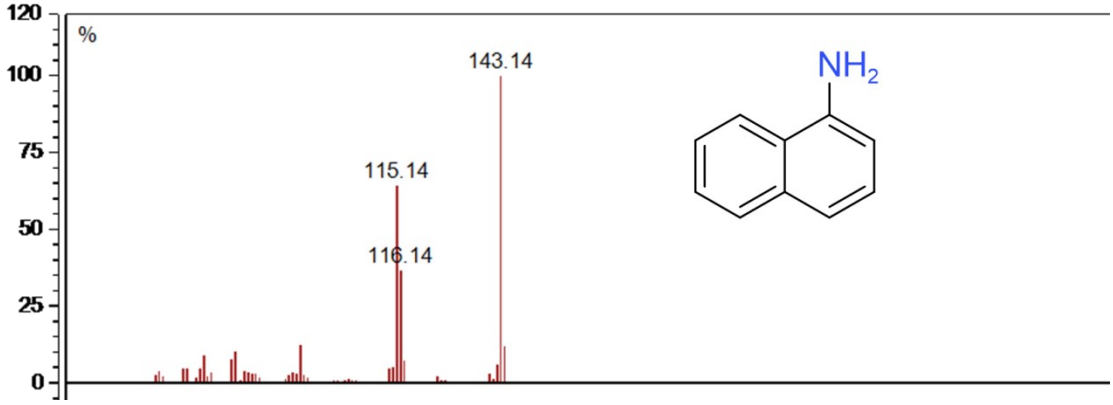

4a: Quinoline

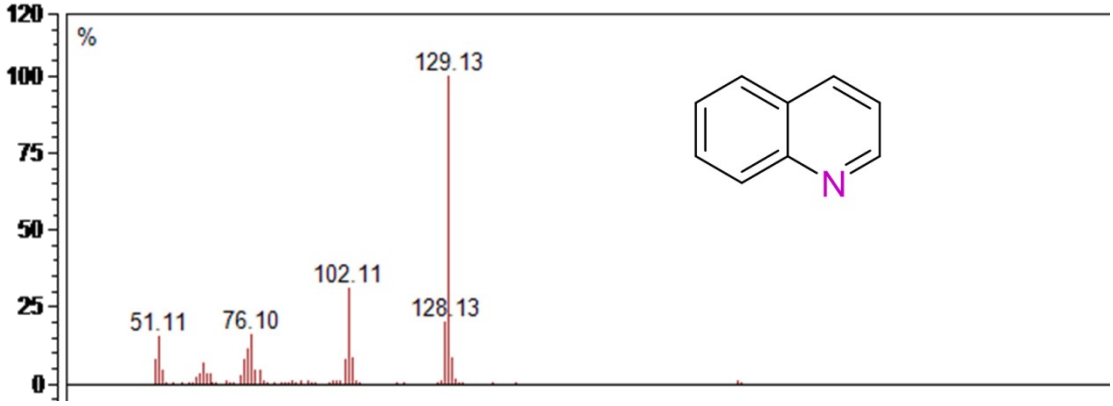

8a: Isoquinoline

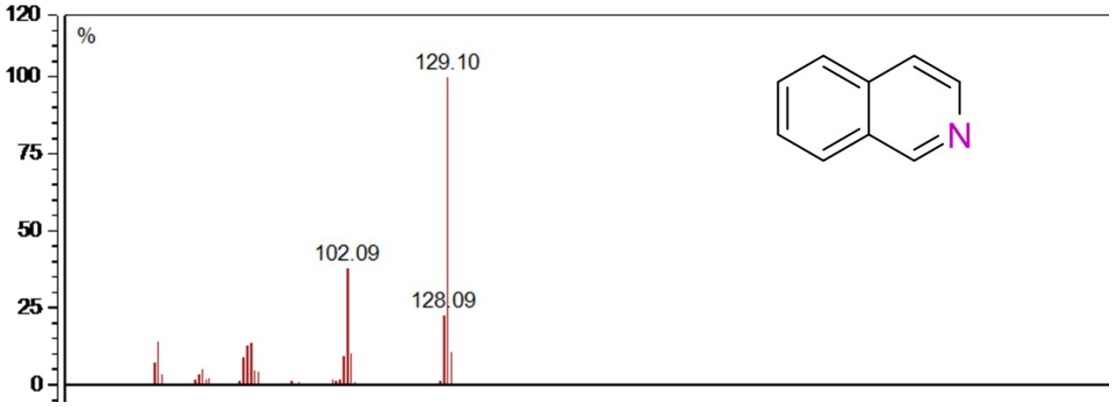

8c: 6-Methylquinoline

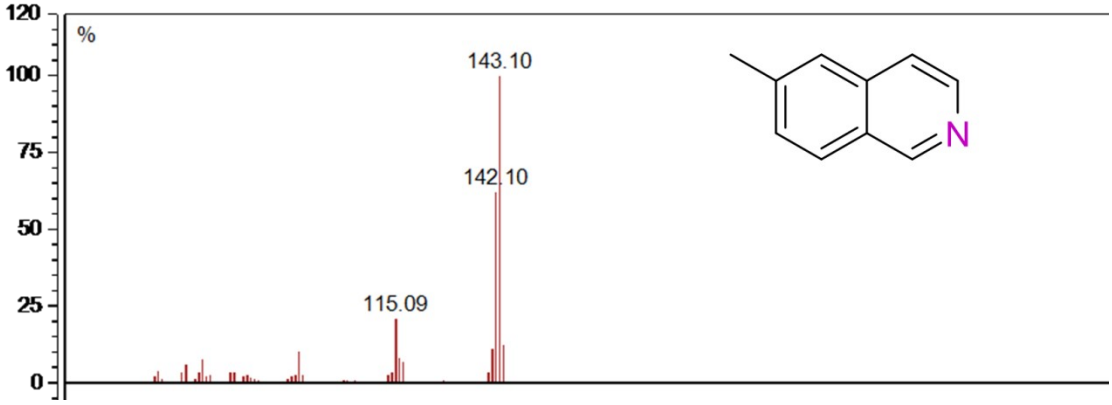

8d: 6-fluoroquinoline

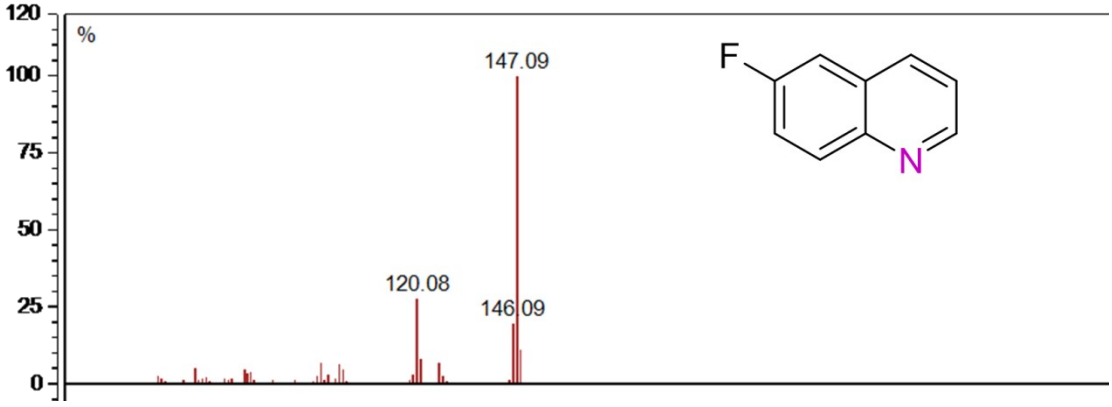

8e: 5-Bromoquinoline

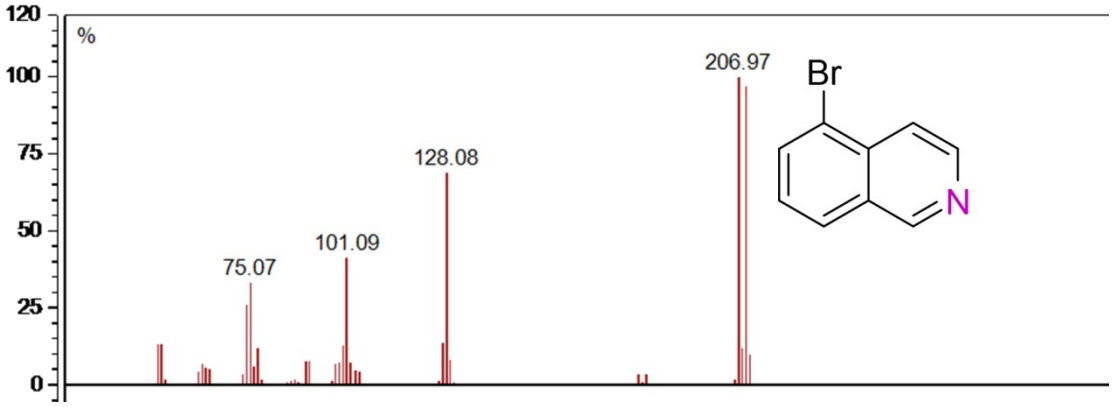

8g: 6-Methoxyquinoline

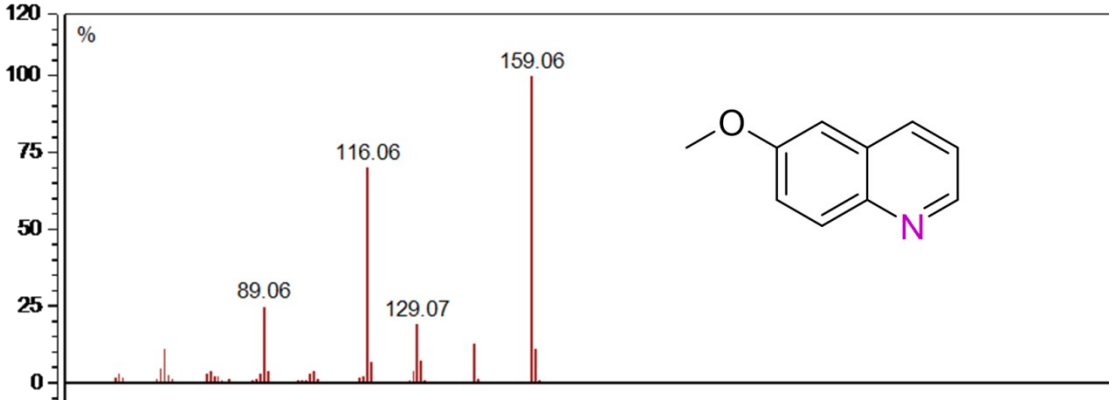

8h: Quinoxaline

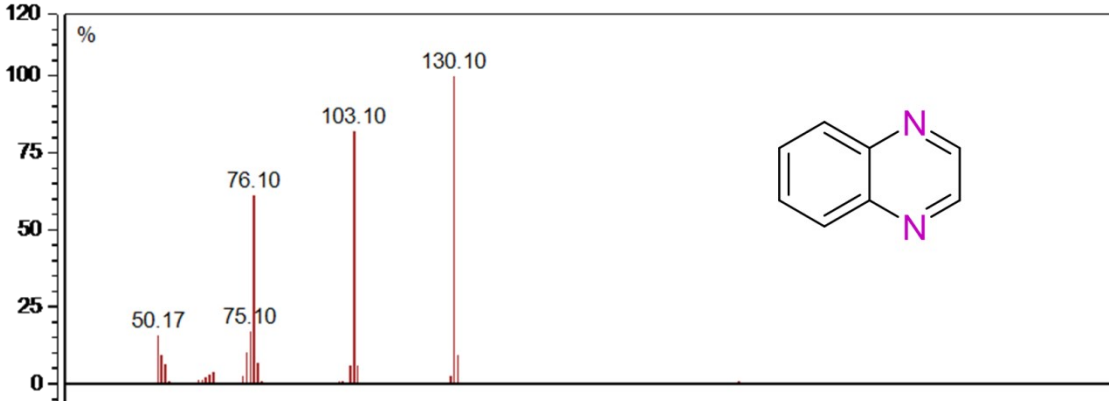

8j: 2-Methylindole

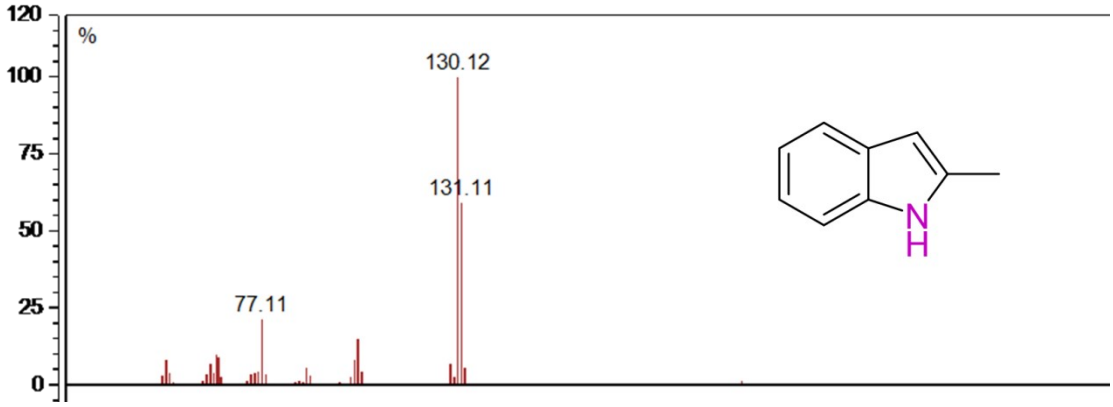

8k: Phenylisoquinoline